# Modeling of Diffusion-Collection Mechanisms in Semiconductor Devices Submitted to Ionizing Radiation

Daniela Munteanu, Jean-Luc Autran

Chapter

# Modeling of Diffusion-Collection Mechanisms in Semiconductor Devices Submitted to Ionizing Radiation

*Daniela Munteanu and Jean-Luc Autran*

## Abstract

When an ionizing particle passes through a semiconductor device, it transfers energy and generates electron-hole pairs along its path. The excess carriers are subsequently transported throughout the semiconductor's volume via ambipolar diffusion until they either recombine or are collected and extracted typically by a biased contact or a reverse-biased p-n junction. To predict the transient electrical behavior of complementary metal-oxide semiconductor (CMOS) devices and circuits when exposed to ionizing radiation and assess their soft error rate (SER), it is fundamental to accurately model these diverse physical processes. In this chapter, we present a comprehensive modeling and analysis of the diffusion and collection mechanisms of radiation-induced charges through a semiconductor device. Analytical formulations of the collected charge, collection current, and collection velocity are developed. These equations are further employed to establish an analytical formulation of the soft error rate (SER), explaining its exponential dependence on the critical charge of the circuit. This formulation also links the SER to various physical and technological parameters, as well as to the characteristics of the radiation.

**Keywords:** complementary metal-oxide semiconductor (CMOS), critical charge, diffusion-collection, metal-oxide-semiconductor field-effect transistor (MOSFET), radiation effects, semiconductor, single event effects (SEE), soft error rate (SER)

## 1. Introduction

The Earth is constantly exposed to a continuous bombardment of cosmic rays, also known as primary cosmic rays. These cosmic rays are a mixture of highly charged, energetic particles, consisting mainly of protons, helium nuclei, and heavy ions [1]. They come from various regions of deep space as well as from the Sun and arrive at Earth from all directions [2]. In the Earth's upper atmosphere, the primary cosmic rays interact with atmospheric particles. The result is the formation of extended atmospheric showers, which produces secondary particles that reach sea level. At ground

level, this produces a continuous flow of energy-distributed particles. Some of these particles (such as muons, neutrons, protons, and pions) interact with the materials of electronic devices and circuits and can cause undesirable effects on their operation or performances [3]. An important category of effects consists of single-event effects (SEEs), defined as any measurable or observable change in the state, operation, or performance of a microelectronic device, element, subsystem, or system (digital or analog), resulting from the impact of a single energetic particle [4].

An SEE is always triggered by the interaction of an incident particle with the target material. During the interaction, the incident particle necessarily transfers energy to the medium by electromagnetic or nuclear processes. As a result of these processes, some or all of the energy of the incident particles is released into the medium [5].

There are three main sequential steps involved in the production of SEE in microelectronic devices. The first step is the charge deposition as a result of the particle hitting the sensitive region of the device by one of two mechanisms: direct or indirect ionization [6]. Direct ionization involves charged particles interacting primarily with the electrons of the material's atoms. A large number of excited energetic electrons (delta rays), usually energetic enough to ionize other atoms, are produced by the ionization mechanism. These electrons produce a cascade of secondary electrons, which lose their energy and create electron-hole pairs along the path of the particle. In this way, the deposited energy is essentially converted into electron-hole pairs. The energy required to create an electron-hole pair depends on the band gap of the material. In a silicon substrate, one electron-hole pair is created for every 3.6 eV of energy lost by the particle. Other particles (e.g., neutrons) do not ionize the matter they pass through and do not interact directly with the material. However, these particles can produce SEEs because they are likely to undergo nuclear reactions with atoms in the material. This mechanism is known as indirect ionization. The result of these nuclear reactions is the production of recoils and fragments that, like the charged particles, can deposit energy along their path by direct ionization [6].

The second step in the production of SEEs is the transport of the charge produced in the dense column of electron-hole pairs. Charges are transported by two main mechanisms: the drift of the charge in the regions subjected to an electric field and the ambipolar diffusion of the charge in the neutral zones. Finally, carriers generated in the electron-hole pair column can undergo an additional physical mechanism: carrier recombination with other mobile carriers in the lattice.

The third step is the collection of transported charges by elementary structures in the device (such as biased contacts or reverse-biased junctions). This charge collection process causes a parasitic transient current to be generated. This current is then injected into the node of the circuit affected by the particle and can cause disturbances in the circuit operation, such as SEEs.

Accurate modeling of these diverse physical processes is essential to predict the transient electrical behavior of complementary metal-oxide semiconductor (CMOS) devices and circuits when exposed to ionizing radiation and to assess their soft error rate (SER). The SER is defined as the probability that an ionizing particle will cause a transient error in the circuit that affects its operation, without causing permanent damage [3, 6]. In this chapter, we focus on the mechanisms of diffusion and collection of charges induced by energetic particles interacting with the materials of CMOS devices and circuits. A large amount of simulation and modeling studies have been carried out over the last 40 years in the field of radiation-induced diffusion-collection of charges in CMOS devices [7–21]. However, there are always challenges to be

overcome concerning the calculation of the collection current and the evaluation of the circuit SER. This chapter presents a comprehensive modeling and analysis of radiation-induced charge diffusion and collection mechanisms through a semiconductor device. The aim of our development, based on the fundamental equations of diffusion-collection, is to reexamine some of the established results and to propose a new modeling of the collected charge, the collection current, and the collection velocity. Two different approaches are proposed, depending on the formalisms considered for the collection current: a pure diffusion current or a conduction current that includes a collection velocity. The equations obtained for the collected charge are then used to establish an analytical formulation of the soft error rate (SER), which explains its exponential dependence on the critical charge of the circuit. The chapter is structured as follows: In Section 2, we present the principle of the diffusion-collection model, and we recall the fundamental equations of the diffusion-collection mechanisms of the radiation-induced charges. These equations are the starting point of our modeling. Section 3 presents the diffusion-collection modeling based on the theory of diffusion. We start with the theoretical case of a point source and develop analytical expressions for the carrier density, diffusion current, and collected charge. The model accuracy is then verified using random-walk drift-diffusion (RWDD) numerical simulation. Next, we consider the more realistic case of charges that are generated along the path of an ionizing particle with a constant linear energy deposition, and we study the diffusion-collection of these charges. A linear distribution of point charges is used to emulate the particle track. An analytical formulation of the collected charge is proposed and validated through RWDD simulation. The collected charge model is then used to calculate the SER. In Section 4, the modeling of the collected charge and current is developed within a formalism that includes a collection velocity. After presenting the general case of a time- and position-dependent collection velocity, we focus on two particular cases: a time-independent collection velocity and a constant collection velocity. In the latter case, we show that the exponential form of the SER, which has long been established empirically in the literature, can be obtained analytically. It relates the SER to various physical and technological parameters and the characteristics of the radiation.

## 2. Principle of diffusion-collection modeling

As explained in the introduction, when a charged particle traverses through a semiconductor material, the energy it releases is transformed into electron-hole pairs. In the framework of the diffusion-collection model, these pairs are then organized into a series of localized point charges, such as discrete clusters of electrons and holes, concentrated within very tiny regions of the semiconductor material and distributed along the particle track (**Figure 1**). The number of pairs immediately after the energy deposition and pair formation is denoted as $\delta_n$ and $\delta_p$ for electrons and holes, respectively, with $\delta_n = \delta_p = \delta n_0$.

The physical mechanism through which these excess charges (electrons and holes) are transported is ambipolar diffusion, particularly in the neutral zones of the device where there is no electric field. The model then assumes that a three-dimensional (3D) spherical diffusion law in the semiconductor domain governs the transport of these excess carriers. In the case of electrons, the time and space variation of the excess electron density $n_e$ ($m^{-3}$) is given by the following equation [8]:

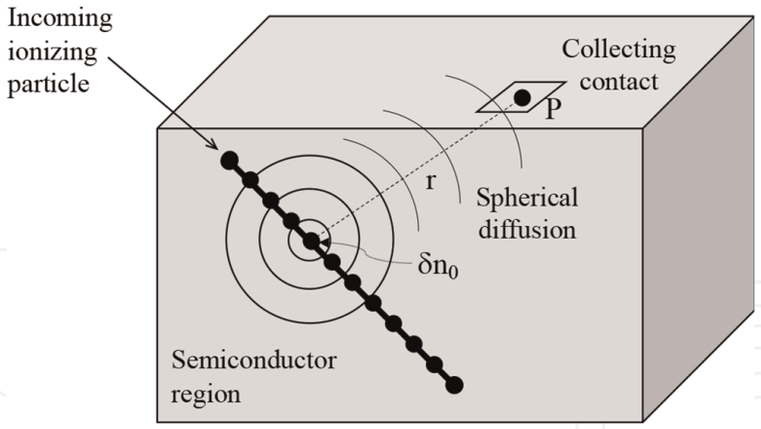


**Figure 1.**
*Principle of the diffusion-collection modeling of radiation-induced charges.*

$$\frac{\partial n_e(r,t)}{\partial t} - \frac{n_e(r,t)}{\tau} = D\nabla^2 n_e \tag{1}$$

where $\tau$ is the electron lifetime, and $D$ is the ambipolar diffusion coefficient. $D$ is obtained from $D_n$ and $D_p$, the diffusion coefficients for electrons and holes, respectively, as follows:

$$D = \frac{2D_n D_p}{D_n + D_p} \tag{2}$$

The solution of Eq. (1) gives the excess carrier density at the time $t$ at a distance $r$ from the point of the initial charge deposition as follows:

$$n_e(t,r) = \frac{\delta n_0}{(4\pi Dt)^{\frac{3}{2}}} e^{\left(-\frac{r^2}{4Dt} - \frac{t}{\tau}\right)} \tag{3}$$

To maintain the analytical nature of the model, we neglect carrier recombination in Eq. (3). This is an important approximation, but it simplifies the calculations in the following to a considerable extent. The new excess carrier density equation is as follows:

$$n_e(t,r) = \frac{\delta n_0}{(4\pi Dt)^{\frac{3}{2}}} e^{-\frac{r^2}{4Dt}} \tag{4}$$

As explained above, the charge transported by ambipolar diffusion is then collected by collecting structures of CMOS devices. The charge collected at point $P$ (**Figure 1**) by a small surface contact, which does not develop an electric field in the semiconductor, can be evaluated using Eq. (4). The charge is calculated by integrating the current density at point $P$ over the surface of the contact and over time, from 0 to infinity. At this point, two different formalisms can be chosen to evaluate the current density: the theory of diffusion or the general electrokinetic formulation of the conduction. In the following, we present models of collected charge, collected current, and SER, using both formalisms successively.

*DOI: http://dx.doi.org/10.5772/intechopen.1003991*

## 3. Diffusion-collection modeling based on the theory of diffusion

### 3.1 Collected charge from a point source

We start with the theoretical case of a point source of radiation-induced charges located at $t = 0$ at the $O$ point within the semiconductor, as illustrated in **Figure 2**. The point charge contains a number $\delta n_0$ of carrier in-excess resulting from a punctual energy transfer that creates electron-hole pairs. In the following, we detail only the case of electrons, but the transport of holes can be treated similarly. The charge $q\delta n_0$ is transported by diffusion and the variation in time and space of the excess carrier density is given by Eq. (4) if neglecting the carrier recombination process. To calculate the collected charge at the $P$ point of the collecting contact, we assume in the following that the current density is expressed in the diffusion theory formalism.

#### *3.1.1 Diffusion current and collected charge modeling*

The diffusion current density is given by the following:

$$\overrightarrow{J_{diff}}(r,t) = qD\vec{\nabla}(n_e) \tag{5}$$

The flow of charges transported by diffusion is collected at the surface of the semiconductor by a very small area contact centered at the $P$ point, as shown in **Figure 2**. The integration of the current density (Eq. (5)) over the contact area gives the collected current as follows:

$$I_{diff}(r,t) = \iint_{A_C} \overrightarrow{J_{diff}}(r,t)\,\overrightarrow{dS} \approx qA_C D\frac{\partial n_e(r,t)}{\partial r} \tag{6}$$

where $A_C$ is the contact area. To avoid numerical integration in Eq. (6), we assume that the contact is sufficiently "small" compared to all other geometric dimensions. The diffusion current can also be calculated according to Eq. (6) as follows:

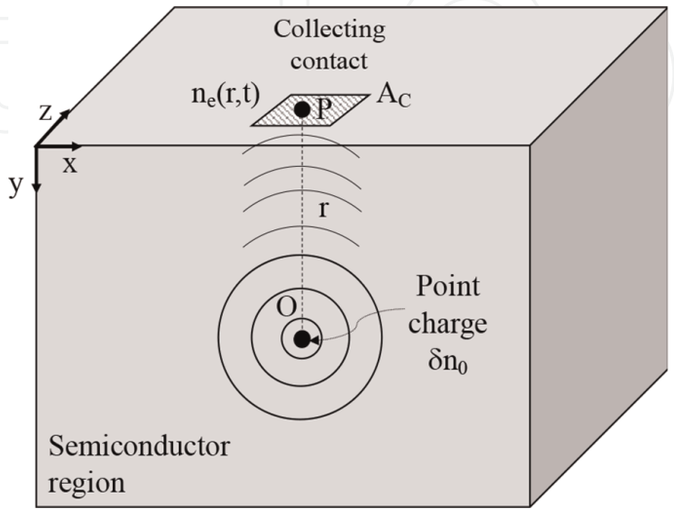


**Figure 2.**
*Schematical illustration of the 3D spherical diffusion of a point charge and collection by a small surface collecting contact.*

$$\left|I_{diff}(r,t)\right| = \frac{qA_C\delta n_0}{(4\pi D)^{\frac{3}{2}}} \times \frac{r}{2t^{\frac{5}{2}}} \times e^{-\frac{r^2}{4Dt}} = qA_C n_e(r,t) \times \frac{r}{2t} \tag{7}$$

From the collected current, the charge collected at the contact at the *P* point can be obtained by integrating Eq. (7) over time as follows:

$$q_{col}^{diff}(r,t) = \int_0^t I_{diff}(r,t')dt' = \frac{qA_C\delta n_0}{2(\pi)^{\frac{3}{2}}r^2} \times \frac{r}{2t^{\frac{5}{2}}} \times \Gamma\left(\frac{3}{2}, \frac{r^2}{4Dt}\right) \tag{8}$$

where Γ(a, x) is the upper incomplete gamma function [22]. As time tends toward infinity, the gamma function in Eq. (8) becomes equal to $\sqrt{\pi}/2$ . In this case, the amount of charge collected reaches its maximum value given by the following:

$$q_{col}^{diff}(r) = q\delta n_0 \times \frac{A_C}{4\pi r^2} \tag{9}$$

The total charge collected at the *P* point, resulting from the initial charge $\delta n_0$ at the *O* point and given by Eq. (9), obviously no longer depends on time but still depends on the distance between the *O* point and the contact.

### *3.1.2 Verification by RWDD numerical simulation*

We performed extensive numerical random walk drift-diffusion simulations to validate the diffusion current and collected charge models presented in Eqs. (7)–(9). These simulations included point sources of particles positioned at various distances from the collecting contact. We recall that the random-walk drift-diffusion (RWDD) model is a particle Monte Carlo technique. It effectively combines drift and diffusion processes using a random-walk algorithm that mimics the Brownian motion [23–25]. In the context of RWDD, the trajectory of an ionizing particle passing through the semiconductor region of devices is represented as a sequence of charge packets distributed along a linear segment. The length of this segment is equal to the range of the ionizing particle within the material. The precision of this charge discretization is guaranteed by adjusting the level of "granularity." This can be fine-tuned by choosing the packet size, which in practice typically ranges from 1 to 100 elementary charges. The transport and the recombination of the electron and hole charge packets begin immediately after the particle passes through the device. Excess carriers undergo both diffusion and drift within the preexisting "background" electric field that existed before the particle impact in the equilibrium state. The drift-diffusion motion from time *t* to *t* + *Δt* of a charge packet located at *r(t)* is calculated as follows [23–25]:

$$r(t+\Delta t) = r(t) + \mu t E_0(r(t)) + N_3(0,1)\sqrt{2D\Delta t} \tag{10}$$

where $\mu$ is the carrier ambipolar mobility, $N_3(0,1)$ is a 3D standard normal random vector (i.e., a triplet of reals between 0 and 1 distributed following the normal distribution [26]), and $E_0$ is the electric field before the particle strike. To account for the simplifying assumptions previously made in current and charge modeling, in the present RWDD simulation, there is no electric field, and the recombination process is neglected. A pure 3D ambipolar diffusion process is then simulated by the numerical code. During each time step of the simulation, the collected current resulting from the

initial radiation-induced charge is calculated based on the transport dynamics of the minority charge packets described by Eq. (10). We use the continuity equation at the collector contact to estimate this collected current. Then, the transient current is directly computed from the number of carriers $\Delta n$ that reach this contact during the time step $\Delta t$ as $I(t) = q \times \Delta n/\Delta t$. More details about this simulation method and its practical implementation using an object-oriented programming language can be found in [23–25].

An illustration of the charge transport simulation after the generation of electron-hole pairs in the particle Monte Carlo RWDD approach is shown in **Figure 3**. In this simulation, we consider a radiation-induced punctual charge $\delta n_0$ of 10,000 electrons located at 1 μm from a collecting contact of surface $A_C = 0.2 \times 0.2\ \mu m^2$. **Figure 3** shows a sequence of four different moments captured at $t$ = 0, 0.1, 1, and 3 ps after the punctual charge generation, visually illustrating the progression of the RWDD charge transport process. Carriers are transported according to a 3D spherical diffusion law in all directions. Some of these carriers that either reach or cross the contact surface during the simulation run are collected at the contact.

We use RWDD simulation to verify and validate the analytical modeling of the collected charge given by Eqs. (8) and (9). **Figure 4** shows the time evolution of the

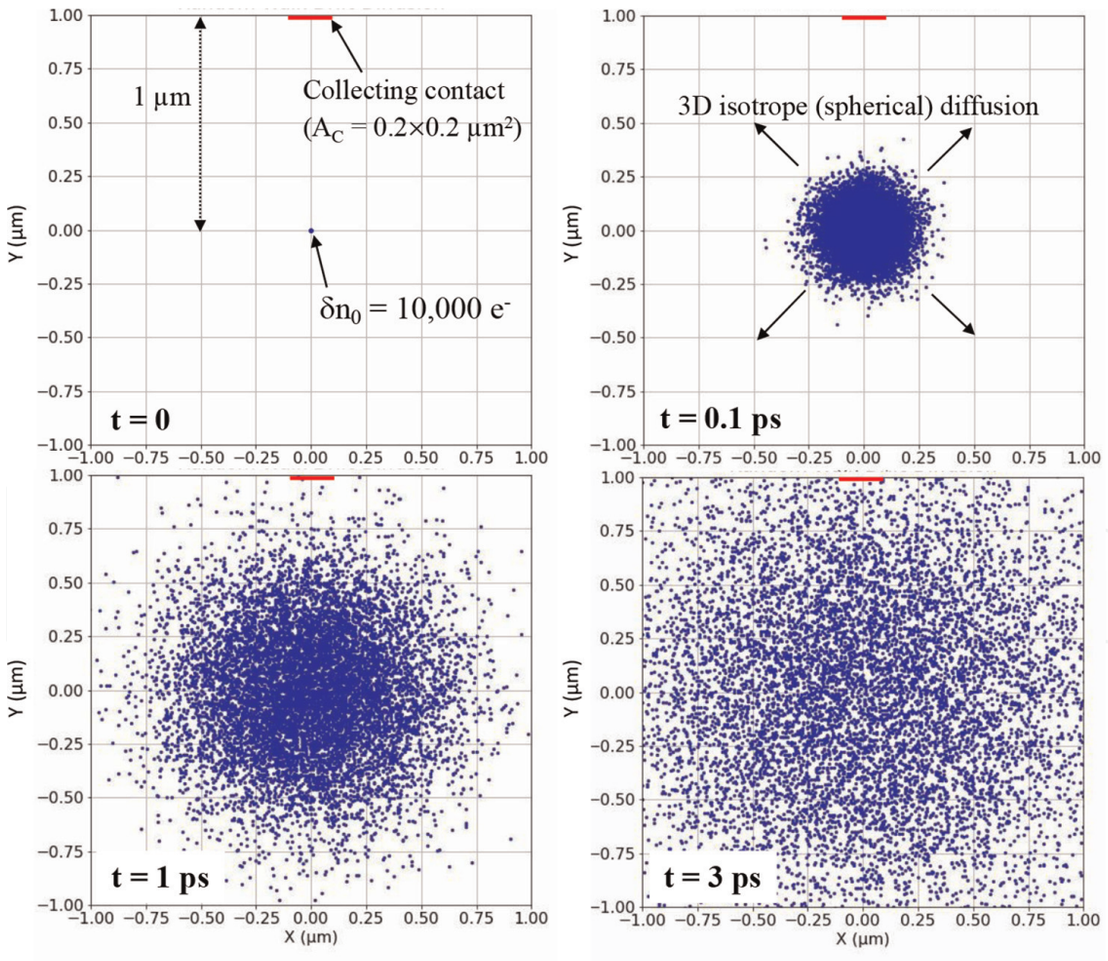


**Figure 3.**
*Distributions of charges in a vertical section along the x-y plane (z = 0) at* t = 0, 0.1, 1 *and 3 ps after the deposition of 10,000 electrons at position (0, 0, 0). Charges are transported following Eq. (10) with* $D^* = 533\ cm^2/s$, $\Delta t = 0.1$ *ps, and* $E_0 = 0$ *(pure diffusion law). The surface of the collecting contact is in the x-z plane, perpendicular to the figure.*

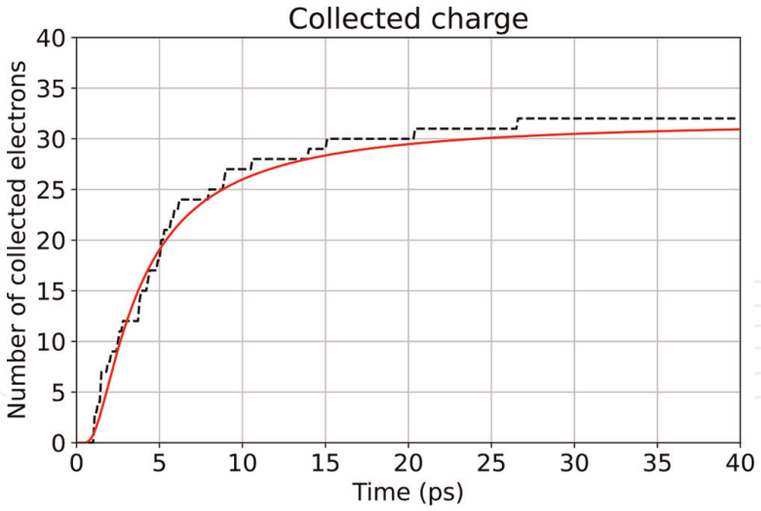


**Figure 4.**
*Time evolution of the charge collected by a small contact ($A_C$ = 0.2 × 0.2 μm²) located at 1 μm from the initial deposition of 10,000 electrons (see **Figure 3**) analytically predicted by Eq. (8) and numerically computed using the Monte Carlo RWDD simulation code.*

charge collected by the contact given by Eq. (8) and by RWDD simulation with the parameters considered in **Figure 3**. We observe good agreement between the two curves shown in **Figure 4**. In addition, the maximum collected charge predicted by Eq. (9) closely matches that obtained in the RWDD simulation. This demonstrates the validity of Eqs. (8) and (9) in describing the time dependence of the collected charge. **Figure 4** also shows the stochastic nature of the RWDD curve due to the small amount of charge collected, which is about a few tens of electrons at the end of the transient.

### 3.2 Collected charge from a particle track

We consider now the more realistic case of charges that are generated along the path of an ionizing particle with a constant linear energy deposition. We examine a simplified scenario, as shown in **Figure 5**, in which an ionizing particle strikes the

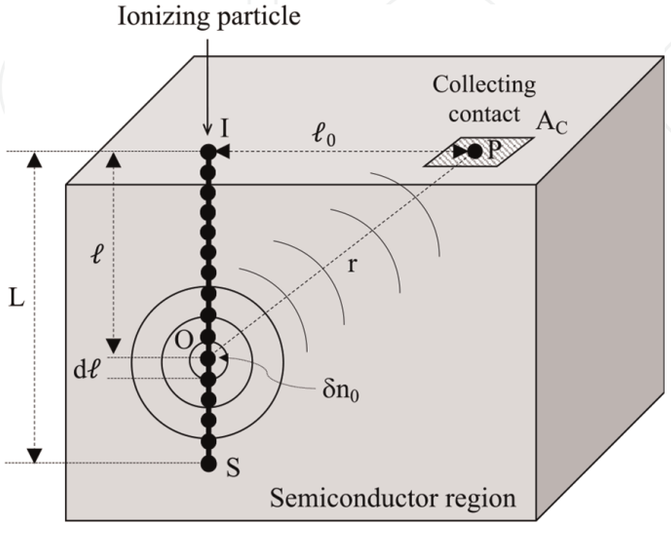


**Figure 5.**
*Schematic representation of a particle impact in the semiconductor region of a circuit. The particle track is treated as a set of point charges $\delta n_o$ uniformly distributed along a straight segment of length L.*

semiconductor surface perpendicularly. It enters the semiconductor at location I, moves through the semiconductor over a path equal to its range, and stops at location S.

The particle loses the energy $\Delta E$ energy along the [IS] segment of length $L$. The particle creates along its track a total number of pairs given by the following:

$$N = \frac{\Delta E}{E_{e,h}} \tag{11}$$

where $E_{e,h}$ is the energy required to create an electron-hole pair in the target semiconductor material.

The particle track is treated as a set of point charges $\delta n_0$ uniformly distributed along the straight segment [IS]. With the particle track divided in this way, the equations developed previously in the case of the diffusion from a point charge can be used here to calculate the collected charge on the contact centered at the P point. In the following, we assume that the particle has a constant LET, which means that the generated charge is deposited uniformly along its track. Under this assumption, each

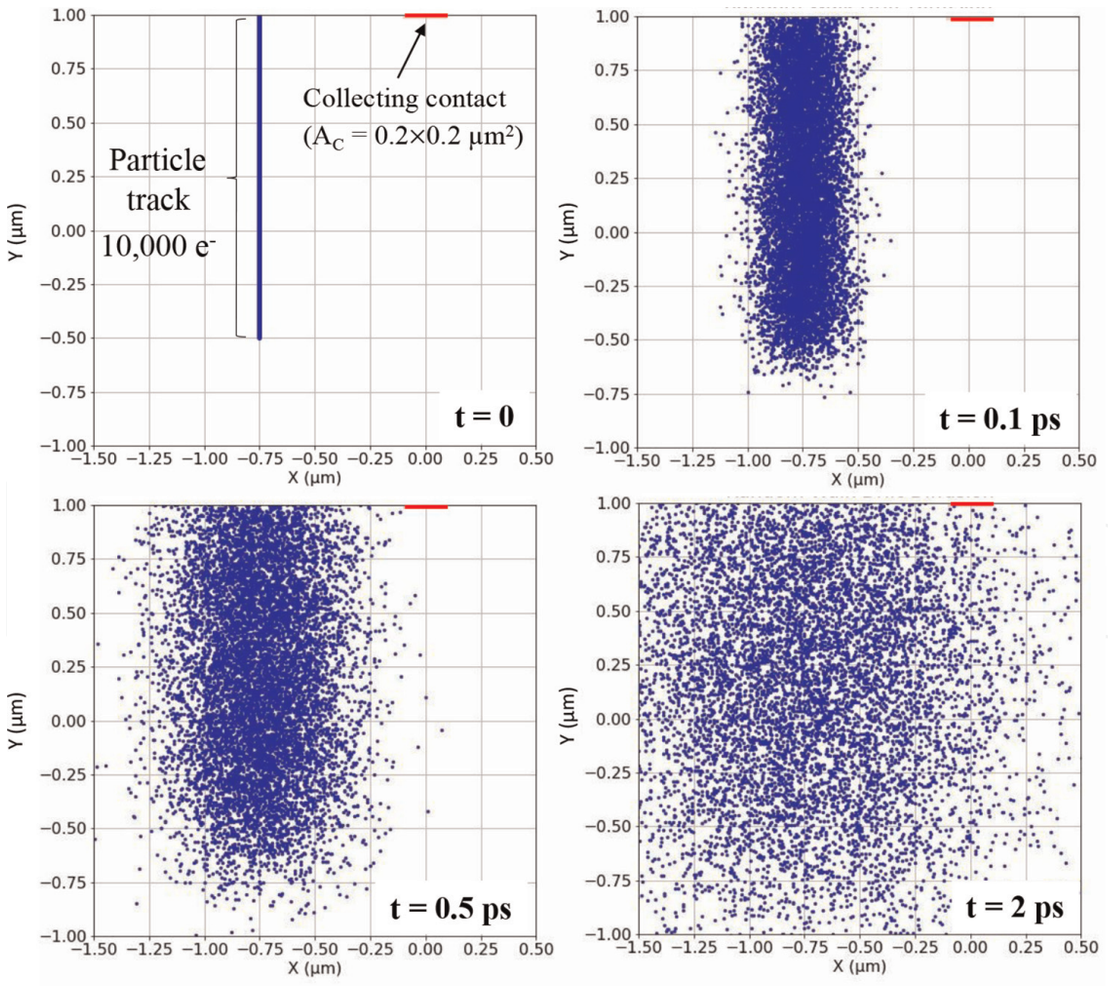


**Figure 6.**
*Distributions of charges in a vertical section along the x-y plane (z = 0) at t = 0, 0.1, 0.5, and 2 ps after the deposition of 10,000 electrons along a 1.5-μm length track located at 0.75 μm from the contact. Other simulation parameters are the same as reported in the caption of* ***Figure 3****.*

elementary segment of length $d\ell$ carries an elementary charge $\delta n_0$ considered punctual. Then, $\delta n_0$ is calculated from the total number of pairs $N$ as follows:

$$\delta n_0 = \frac{N}{L} \times d\ell = \frac{\Delta E}{E_{e,h} L} \times d\ell \tag{12}$$

where $\ell$ and $d\ell$ are defined in **Figure 5**.

The total collected charge at P point, $Q_{col}^{diff}$, can be now calculated by integrating Eq. (9) along the entire particle track, with $r = \sqrt{\ell_0^2 + \ell^2}$ as follows:

$$Q_{col}^{diff} = \frac{qA_C N}{4\pi L} \int_0^L \frac{d\ell}{\ell_0^2 + \ell^2} \tag{13}$$

From (13), the total collected charge at P point is given by the following:

$$Q_{col}^{diff} = Q_0^{diff} \times arctan\left(\frac{L}{\ell_0}\right) \tag{14}$$

with

$$Q_0^{diff} = \frac{qA_C N}{4\pi L \ell_0} \tag{15}$$

Eq. (14) has been validated by RWDD numerical simulation. We have considered an incident particle with a track of 1.5 μm hitting the semiconductor at a distance of 0.75 μm from the contact. A sequence of four different moments captured at $t$ = 0, 0.1, 0.5, and 2 ps after the charge generation is shown in **Figure 6**. As in the case of a point charge, this series of figures shows the transport of the radiation-induced charge by a spherical diffusion law. A part of the diffused charge is finally collected by the small

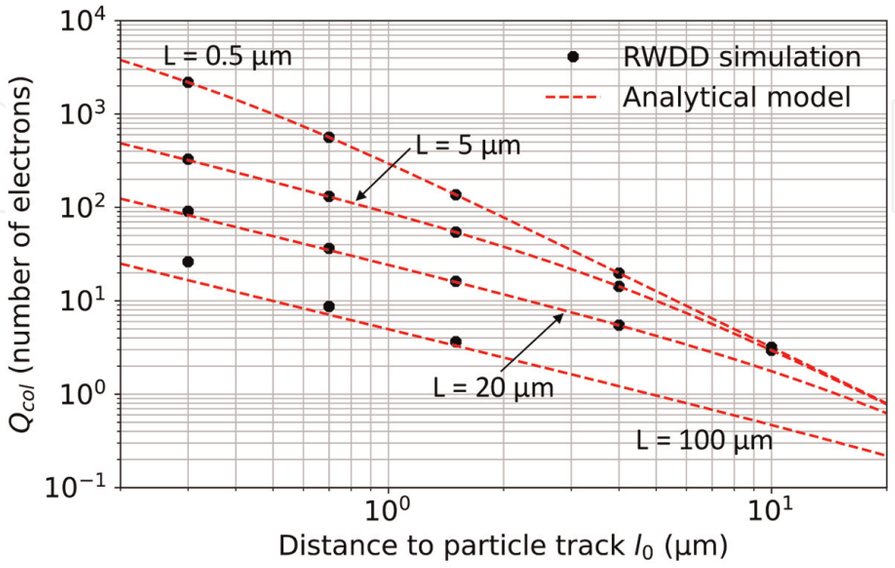


**Figure 7.**
*Collected charge versus the distance $\ell_0$ from the collecting contact to the particle track of length L (see **Figure 5**). The collected charge is analytically calculated using Eq. (14) and numerically computed using the Monte Carlo RWDD simulation code.*

contact area. Next, we have been able to compare the numerical simulation and the analytical model of the collected charge given by Eqs. (14) with (15) through systematic RWDD simulations for different values of $\ell_0$ and $L$. The results are shown in **Figure 7** for four values of the track length $L$. A very good agreement was obtained between the collected charge calculated with the analytical model and that simulated using the Monte-Carlo RWDD code, as shown in **Figure 7**.

### 3.3 SER modeling

To determine the SER of the circuit, we use the notion of critical charge, which is a key parameter for assessing the susceptibility to radiation of the circuit. The critical charge $Q_{crit}$ is the minimum amount of collected charge required to trigger a transition from a logical low to a logical high state or vice versa at a sensitive node of the circuit [3, 6]. In the following, we will focus on the case where the collected charge is equal to the critical charge of the circuit. Eq. (15) shows that the collected charge is a function of the position $\ell_0$ between the track and the contact. We define $\ell_{crit}$ as the distance $\ell_0$ for which $Q_{col}^{diff} = Q_{crit}$ as follows:

$$Q_{col}^{diff} = Q_{crit} = \frac{qA_C N}{4\pi L \ell_{crit}} \times arctan\left(\frac{L}{\ell_{crit}}\right) \tag{16}$$

According to Eq. (16), a particle hitting the semiconductor at a distance $\ell_0$ smaller than $\ell_{crit}$ will result in a collected charge greater than $Q_{crit}$, thus, causing a change of state of the circuit (i.e., an error). Otherwise, a particle track located at a distance greater than $\ell_{crit}$ will not trigger an error. Therefore, the critical surface within which the passage of an ionizing particle will trigger an error is the surface of the disk with a radius equal to $\ell_{crit}$ and centered on the small contact. The SER of the circuit, that is, the rate at which errors occur at the sensitive node defined by the small area contact centered at the P point, can then be calculated from the following eq. [21]:

$$SER = \pi \ell_{crit}^2 F \tag{17}$$

where $F$ is the particle flux (in $m^{-2}\ s^{-1}$).

Usually, the critical charge $Q_{crit}$ is a known value for a given circuit, a value that can be obtained by various types of simulation such as mixed-mode, TCAD, or circuit-level simulations. Using this value in Eq. (16), the value of $\ell_{crit}$ and therefore of the SER can be calculated. Eq. (16) with the unknown $\ell_{crit}$ is a transcendental equation that can be solved numerically to obtain $\ell_{crit}$ but which has no analytical solution. The numerical solving of Eq. (16) can be performed using the dichotomy or Newton-Raphson methods [27].

To express the solution of Eq. (16) analytically, we use a well-known approximation for the arctan function as follows:

$$\arctan(x) \approx \frac{\pi}{2} \times \frac{x}{1 + |x|} \tag{18}$$

We set

$$x = \frac{L}{\ell_{crit}} \tag{19}$$

Then, Eq. (16) becomes.

$$x^2 - Bx - B = 0 \tag{20}$$

where $B$ is given by the following:

$$B = \frac{8L^2 Q_{crit}}{qA_C N} \tag{21}$$

The positive solution of the second-degree polynomial in Eq. (20) directly gives $\ell_{crit}$ as follows:

$$\ell_{crit} = \frac{2L}{B + \sqrt{B^2 + 4B}} \tag{22}$$

The SER can be then calculated from Eqs. (17) and (22) as follows:

$$SER = \pi \ell_{crit}^2 F = \frac{4\pi L^2 F}{\left(B + \sqrt{B^2 + 4B}\right)^2} \tag{23}$$

We have compared the SER given by Eq. (23) with the SER obtained as the exact solution of Eq. (16) solved numerically by the dichotomy method. **Figure 8** shows the results of this comparison for three particle track lengths. In this figure, the SER is plotted as a function of critical charge for both calculation methods. A good agreement between the analytical model and the numerical solution is obtained, in particular for large values of the critical charge.

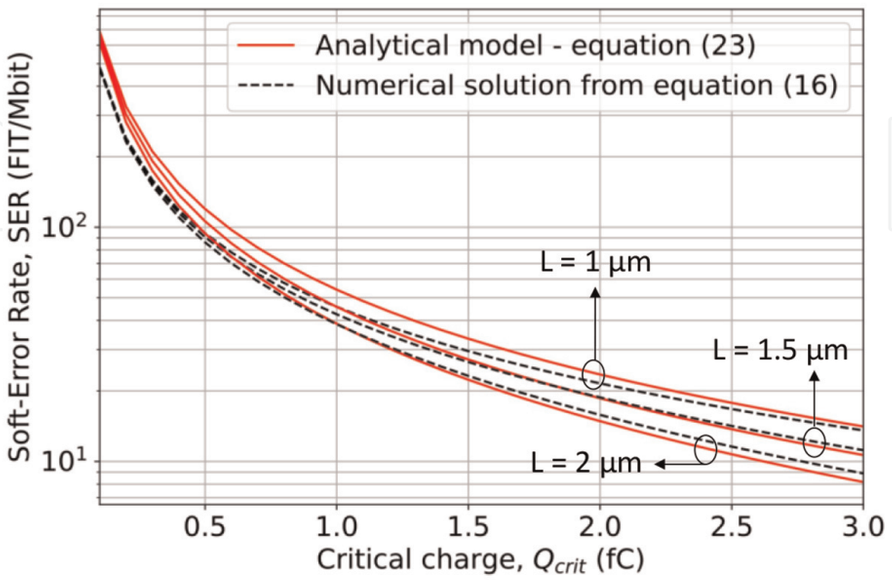


**Figure 8.**
*Soft-error rate as a function of the critical charge calculated from the analytical model of Eq. (23) and from the numerical solving of Eq. (16). Simulation parameters are as follows:* $A_C = 0.1\ \mu m^2$, $N = 1.38 \times 10^6$, $D = 61\ cm^2\ s^{-1}$, *and* $F = 10^{-3}\ cm^{-2}\ h^{-1}$.

## 4. Diffusion-collection based on the collection velocity

As explained before, the general kinetic formulation of conduction is a second formalism that can be used to calculate the density of the current collected at the contact coming from the charges generated along the ionizing particle track. In this section, we will use this formalism to express the current density and the collected charge, as well as the SER of the circuit. This formalism introduces the notion of collecting velocity, which leads to several approximations related to its dependence on time and space, as we will see below.

### 4.1 Conduction current

In the general kinetic formulation of conduction, the current density is given by the following:

$$\overrightarrow{J_{cond}} = qn\vec{v} \tag{24}$$

where $n$ is the electron density, and $v$ is the electron diffusion velocity. We use Eq. (24) for the carriers of density $n_e$ transported by diffusion from the particle track to the P point. These carriers are collected by crossing the collection surface of the contact in the absence of an electric field and are uniquely transported by the diffusion process. Their diffusion velocity is therefore referred to as $v_{col}$ for "collection velocity." The collected current is obtained by integrating Eq. (24) over the surface $A_C$ of the collected contact as follows:

$$I_{cond}(r,t) = qA_C v_{col}(r,t) n_e(r,t) \tag{25}$$

The current density, whether expressed in diffusion theory or in the general formulation of conduction theory, must be the same. Therefore, Eqs. (5) and (24) must be equal as follows:

$$qD\vec{\nabla}(n_e) = qn_e\overrightarrow{v_{col}} \tag{26}$$

which results in the following equation for the collection velocity:

$$\overrightarrow{v_{col}} = D\frac{\vec{\nabla}(n_e)}{n_e} \tag{27}$$

From Eq. (27), $v_{col}$ can be also rewritten as follows:

$$v_{col}(r,t) = \frac{r}{2t} \tag{28}$$

Eq. (28), which gives the general formula for the collection velocity, indicates that $v_{col}$ depends on both the time and the distance between the particle track and the charge collection contact. Inserting the collection velocity expression (28) into Eq. (25) gives the collection current as follows:

$$I_{cond}(r,t) = qA_C n_e(r,t) \times \frac{r}{2t} \tag{29}$$

It is obvious that integrating the collection current given by Eq. (29) over time from 0 to infinity will give the same collected charge as that given by Eq. (9). In this case, the calculation of the total charge and the SER will also be the same as that described in the previous section. We therefore obtain the same collected charge using both formalisms for the current density. This is, of course, an expected result. In fact, the interest in using this second formalism based on the collection velocity lies in the fact that several approximations can be made to this collection velocity to simplify the calculation of the collected charge and of the SER. In the following, we will focus on these approximations of the collection velocity.

### 4.2 Time-independent, position-dependent collection velocity

A first approximation used in many studies [10, 13, 14, 19] is to include a time-independent collection velocity in the expression (25) for the collection current as follows:

$$I_{cond}(r,t) = qA_C v_{col}(r) n_e(r,t) \tag{30}$$

where $n_e(r,t)$ is given by Eq. (4). Integrating (30) over time gives the collected charge in the conduction current formalism as follows:

$$q_{col}^{cond}(r,t) = \int_0^t I_{col}(r,t')dt' = \frac{qA_C v_{col}(r)\delta n_0}{4(\pi)^{\frac{3}{2}}Dr} \times \Gamma\left(\frac{1}{2}, \frac{r^2}{4Dt}\right) \tag{31}$$

As time tends toward infinity, the gamma function in Eq. (31) becomes equal to $\sqrt{\pi}$, and the collected charge reaches its maximum value given by the following:

$$q_{col}^{cond}(r) = q\delta n_0 \times \frac{A_C v_{col}(r)}{4\pi Dr} \tag{32}$$

The amount of charge collected given by Eq. (32) must equal the amount of charge given by Eq. (9). This results in the following equation for the collection velocity:

$$v_{col}(r) = \frac{D}{r} \tag{33}$$

As expected, this collection velocity is independent of time and depends only on the position $r$. To simplify the calculations, Eq. (33) can be used to obtain an averaged velocity along the track as follows:

$$v_{col}^{av} = \frac{1}{L} \times \int_0^L \frac{D}{r} d\ell = \frac{D}{L} \times \int_0^L \frac{1}{\sqrt{\ell_0^2 + \ell^2}} d\ell = \frac{D}{L} arsinh\left(\frac{L}{\ell_0}\right) \tag{34}$$

The maximum collected charge given by Eq. (32) becomes:

$$q_{col}^{cond}(r) = \delta n_0 \times \frac{A_C v_{col}^{av}}{4\pi Dr} = q\delta n_0 \times \frac{A_C}{4\pi Lr} arsinh\left(\frac{L}{\ell_0}\right) \tag{35}$$

The total collected charge is obtained, similar to Eq. (13) and using (12), by integrating Eq. (35) along the entire particle track from 0 to $L$ as follows:

$$Q_{col}^{cond} = \frac{qA_C N v_{col}^{av}}{4\pi DL}\int_0^L \frac{d\ell}{\sqrt{\ell_0^2+\ell^2}} = \frac{qA_C N}{4\pi L^2} \times \left[arsinh\left(\frac{L}{\ell_0}\right)\right]^2 \tag{36}$$

The total collected charge is then given by the following:

$$Q_{col}^{cond} = Q_0 \times \left[arsinh\left(\frac{L}{\ell_0}\right)\right]^2 \tag{37}$$

where

$$Q_0 = \frac{qA_C N}{4\pi L^2} \tag{38}$$

Next, we calculate the SER according to the relation (17) in the same way as in Section 3.3. The length $\ell_{crit}$ is obtained by setting the condition $Q_{col}^{cond} = Q_{crit}$ in Eq. (37), which leads to the following equation for $\ell_{crit}$:

$$\ell_{crit} = \frac{L}{sinh\left(\sqrt{\frac{Q_{crit}}{Q_0}}\right)} \tag{39}$$

The SER can be then calculated from Eqs. (17) and (39) as follows:

$$SER = \pi\ell_{crit}^2 F = \frac{\pi L^2 F}{\left[sinh\left(\sqrt{\frac{Q_{crit}}{Q_0}}\right)\right]^2} \tag{40}$$

The SER derived from Eq. (40) and that calculated by the numerical solving of Eq. (16) were compared in detail, as shown in **Figure 9**. Three values of particle track length were considered in this figure. A very good agreement between the analytical model and the numerical solution is observed over the whole range of critical charge values. This shows that assuming a time-independent collection velocity with a value averaged over the track length leads to an acceptable approximation of the SER compared to the exact numerical solution. The advantage of this assumption is that it simplifies the calculation of the SER and provides an analytical solution.

### 4.3 Constant collection velocity

A second approximation, more restrictive than the previous one, is to consider a constant collection velocity (a single numerical value that therefore does not depend on time or position) in the expression of the collected charge (32) [21]. We denote as $v_{COL}$ this constant velocity. Eq. (32) becomes as follows:

$$q_{col}^{cond}(r) = q\delta n_0 \times \frac{A_C v_{COL}}{4\pi Dr} \tag{41}$$

The total collected charge is obtained by integrating Eq. (41) along the entire particle track from 0 to $L$ as follows:

$$Q_{col}^{cond} = \frac{qA_C N v_{COL}}{4\pi DL}\int_0^L \frac{d\ell}{\sqrt{\ell_0^2+\ell^2}} = Q_0 \times arsinh\left(\frac{L}{\ell_0}\right) \tag{42}$$

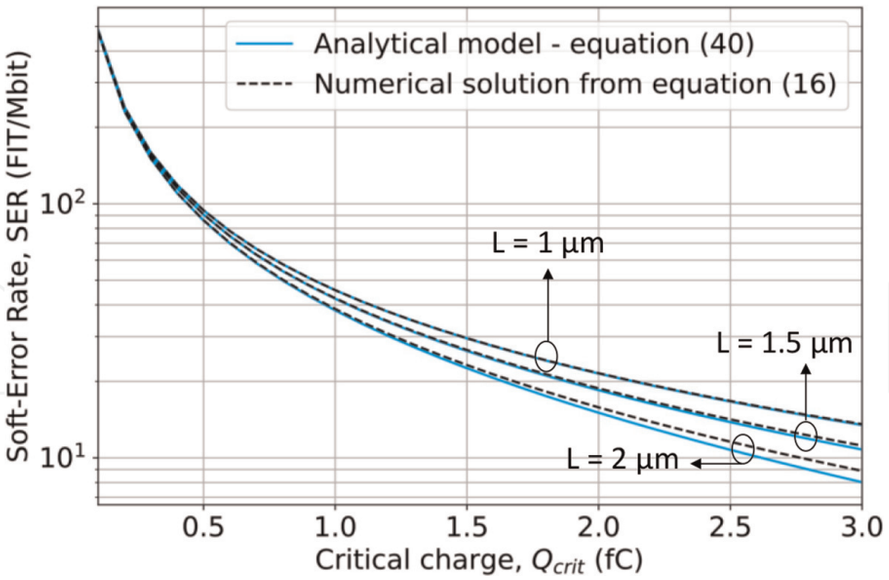


**Figure 9.**
*Soft-error rate as a function of the critical charge calculated from the analytical model of Eq. (40) and from the numerical solving of Eq. (16). Simulation parameters are as follows: $A_C = 0.1\ \mu m^2$, $N = 1.38 \times 10^6$, $D = 61\ cm^2\ s^{-1}$, and $F = 10^{-3}\ cm^{-2}\ h^{-1}$.*

where

$$Q_0 = \frac{qA_C N v_{COL}}{4\pi DL} \tag{43}$$

The next step is to calculate $\ell_{crit}$ that is obtained by setting the condition $Q_{col}^{cond} = Q_{crit}$ in Eq. (42), as explained in the previous sections. The length $\ell_{crit}$ is given in this case by [21] the following:

$$\ell_{crit} = \frac{L}{sinh\left(\frac{Q_{crit}}{Q_0}\right)} \tag{44}$$

Finally, the SER can be calculated from Eqs. (17) and (44) as [21]:

$$SER = \pi \ell_{crit}^2 F = \frac{\pi L^2 F}{\left[sinh\left(\frac{Q_{crit}}{Q_0}\right)\right]^2} \tag{45}$$

As explained in [21], the expression of the SER (45) including a constant value for the collection velocity makes it possible to mathematically demonstrate the exponential dependence of the SER on the critical charge, proposed more than 20 years ago by Hazucha and Svensson in [28] as follows:

$$SER = kFA_C \times e^{-\frac{Q_{crit}}{Q_S}} \tag{46}$$

where $\kappa$ and $Q_S$ are two fitting parameters. This SER formula has been established empirically based on experimental data and is used extensively in the field of SEEs in CMOS circuits. This formula was demonstrated in [21] starting from the fundamental equations of diffusion-collection. Indeed, in Eq. (44), the *sinh* function can be written as follows:

$$sinh\,(x) = \frac{e^{x} - e^{-x}}{2} \tag{47}$$

Assuming that $Q_{crit} \gg Q_0$, Eq. (44) becomes as follows:

$$\ell_{crit} = 2L \times e^{-\frac{Q_{crit}}{Q_0}} \tag{48}$$

and then the SER is given in this case by the following:

$$SER = 4\pi L^2 F \times e^{-\frac{Q_{crit}}{Q_0/2}} \tag{49}$$

Thus, we find an exponential dependence of the SER on the critical charge such as that of Eq. (44) that has been proposed empirically in the literature [28]. Eq. (49) clearly shows that this exponential dependence has a physical basis, being the result of the collection-diffusion mechanism of radiation-induced charges in the semiconductor.

In **Figure 10**, we compare the SER calculated by the exponential expression (49) with the SER obtained by the numerical solution of Eq. (16). We observe that the exponential expression matches the exact value of SER over a limited range of critical charge values (between 1.2 and 2.1 fC for $L$ = 1.5 μm). This range varies as a function of track length, and the collection velocity $v_{COL}$ can be considered as a fitting parameter in this case.

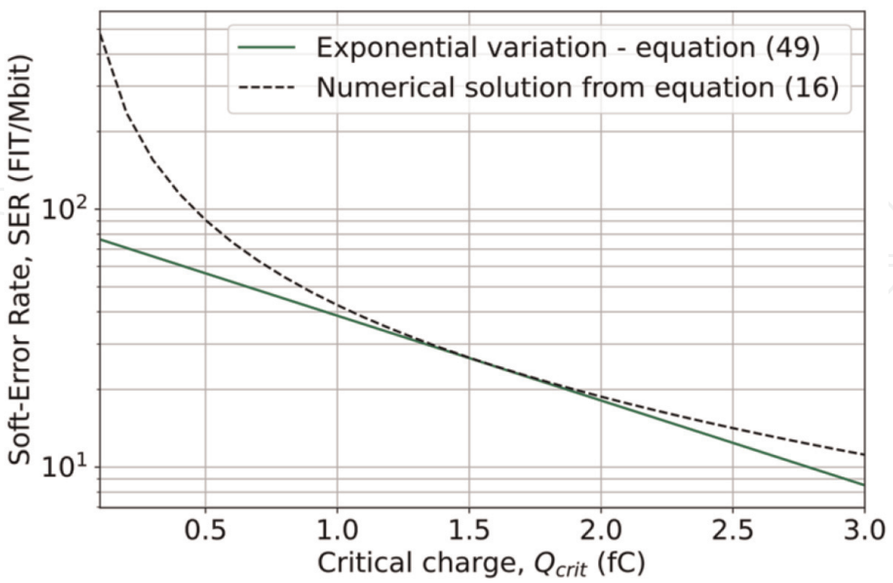


**Figure 10.**
*Soft-error rate as a function of the critical charge calculated from the analytical model of Eq. (49) and from the numerical solving of Eq. (16). Simulation parameters are as follows: $A_C$ = 0.1 μm², L = 1.5 μm, N = 1.3 8 × 10⁶, D = 61 cm² s⁻¹, F = 10⁻³ cm⁻² h⁻¹, and $v_{COL}$ = 4.6 × 10⁵ cm s⁻¹ (in Eq. (49)).*

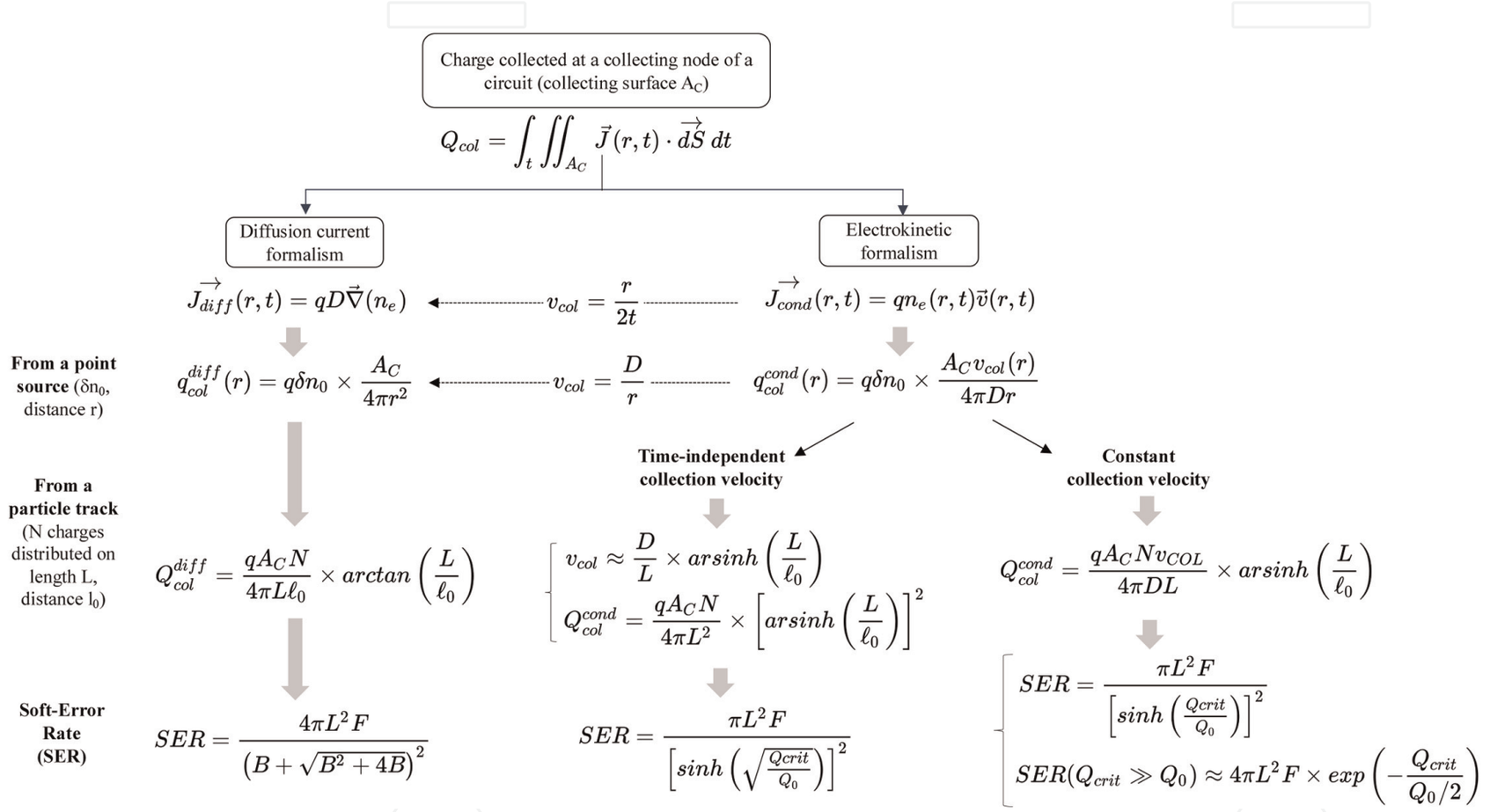


**Figure 11.**
*Summary of the diffusion-collection model developed in this work.*

*DOI: http://dx.doi.org/10.5772/intechopen.1003991*

## 5. Conclusion

In this chapter, we presented a comprehensive modeling and analysis of the mechanisms of radiation-induced charge diffusion and collection through a semiconductor device. Our development proposes a new model of the collected charge, collection current, collection velocity, and soft error rate based on the fundamental diffusion-collection equations. The successive stages of the development are summarized in **Figure 11**, including the most important equations of the model. As shown in this figure, we have considered two different formalisms for the collection current: a pure diffusion current and a conduction current that includes a collection velocity. First, we considered the theoretical case of a point charge source and developed a model for the charge collected by a small contact. Second, this charge was used to model the charge collected in the more realistic case of charges generated along the track of an ionized particle crossing the device. The equations obtained for the collected charge were then used to establish an analytical formulation of the error rate as a function of the critical charge of the circuit. Two approximations can be used to simplify the calculations and obtain analytical expressions in the case of the formalism that includes a collection velocity. A first approximation is the use of a time-independent collection velocity and the integration of an average of this velocity along the particle track into the expression for the collected charge. Our results showed that this assumption leads to an acceptable approximation of the SER compared to the exact numerical solution. A second approximation is the use of a constant collection velocity, which results in an analytical expression of the SER with an exponential dependence on the critical charge. This type of dependence has been proposed empirically in previous works. Our model showed that there is a physical basis for this exponential expression, which results from the charge collection and diffusion mechanism of the radiation-induced charges in the semiconductor.

## Author details

Daniela Munteanu[1*] and Jean-Luc Autran[1,2]

1 Aix-Marseille University, CNRS, IM2NP, Marseille Cedex 20, France

2 University of Rennes, CNRS, IPR (UMR 6251), Rennes Cedex, France

*Address all correspondence to: daniela.munteanu@univ-amu.fr

## References

[1] Valkovic V. Radioactivity in the Environment. Amsterdam: Elsevier; 2000

[2] Dorman LI. Cosmic Rays in the Earth's Atmosphere and Underground. Dordrecht: Kluwer Academic Publishers; 2004

[3] Autran JL, Munteanu D. Soft Errors: From Particles to Circuits. Boca Raton: CRC Press; 2015

[4] JEDEC Standard. Measurement and reporting of alpha particle and terrestrial cosmic ray-induced soft errors in semiconductor devices. N° JESD89B, Revision of JESD89A. 2021

[5] Leroy C, Rancoita PG. Principles of Radiation Interaction Matter and Detection. Singapore: World Scientific Publishing Co. Pte. Ltd; 2004

[6] Munteanu D, Autran JL. Modeling and simulation of single-event effects in digital devices and ICs. IEEE Transactions on Nuclear Science. 2008; **55**:1854-1878

[7] Kirkpatrick S. Modeling diffusion and collection of charge from ionizing radiation in silicon devices. IEEE Transactions on Electron Devices. 1979; **26**:1742-1753

[8] Messenger GC. Collection of charge on junction nodes from ion tracks. IEEE Transactions on Nuclear Science. 1982; **29**:2024-2031

[9] Edmonds L. Charged collected by diffusion from an ion track under mixed boundary conditions. IEEE Transactions on Nuclear Science. 1991;**38**:834-837

[10] Palau JM, Hubert G, Coulie K, Sagnes B, Calvet M-C, Fourtine S. Device simulation study of the SEU sensitivity of SRAMs to internal ion tracks generated by nuclear reactions. IEEE Transactions on Nuclear Science. 2001; **48**:225-231

[11] Palau JM, Wrobel R, Castellani-Coulie K, Calvet M-C, Dodd P, Sexton F. Monte Carlo exploration of neutron-induced SEU-sensitive volumes in SRAMs. IEEE Transactions on Nuclear Science. 2002;**49**:3075-3081

[12] Lambert D, Baggio J, Ferlet-Cavrois V, Flament O, Saigne F, Sagnes B, et al. Neutron-induced SEU in bulk SRAMs in terrestrial environment: Simulations and experiments. IEEE Transactions on Nuclear Science. 2004;**51**:3435-3441

[13] Merelle T, Chabane H, Palau JM, Castellani-Coulie K, Wrobel F, Saigne F, et al. Criterion for SEU occurrence in SRAM deduced from circuit and device simulations in case of neutron-induced SER. IEEE Transactions on Nuclear Science. 2005;**52**:1148-1155

[14] Wrobel F, Hubert G, Iacconi P. A semi-empirical approach for heavy ion SEU cross section calculations. IEEE Transactions on Nuclear Science. 2006; **53**:3271-3276

[15] Correas V, Saigne F, Sagnes B, Boch J, Gasiot G, Giot D, et al. Innovative simulations of heavy ion cross sections in 130 nm CMOS SRAM. IEEE Transactions on Nuclear Science. 2007;**54**:2413-2418

[16] Correas V, Saigne F, Sagnes B, Boch J, Gasiot G, Giot D, et al. Simulation tool for the prediction of heavy ion cross section of innovative 130-nm SRAMs. IEEE Transactions on Nuclear Science. 2008;**55**: 2036-2041

[17] Artola L, Hubert G, Duzellier S, Bezerra F. Collected charge analysis for a new transient model by TCAD simulation in 90 nm technology. IEEE Transactions on Nuclear Science. 2010; **57**:1869-1875

[18] Uznanski S, Gasiot G, Roche P, Tavernier C, Autran JL. Single event upset and multiple cell upset modeling in commercial bulk 65-nm CMOS SRAMs and flip-flops. IEEE Transactions on Nuclear Science. 2010;**57**:1876-1883

[19] Artola L, Hubert G, Warren KM, Gaillardin M, Schrimpf RD, Reed RA, et al. SEU prediction from SET modeling using multi-node collection in bulk transistors and SRAMs down to the 65 nm technology node. IEEE Transactions on Nuclear Science. 2011;**58**:1338-1346

[20] Martinie S, Autran JL, Sauze S, Munteanu D, Uznanski S, Roche P, et al. Underground experiment and modeling of alpha emitters induced soft-error rate in CMOS 65 nm SRAM. IEEE Transactions on Nuclear Science. 2012; **59**:1048-1053

[21] Autran JL, Munteanu D. Physics-based analytical formulation of the soft error rate in CMOS circuits. IEEE Transactions on Nuclear Science. 2023; **70**:782-791

[22] Paris RB. Incomplete gamma and related functions. In: Olver FWJ, Lozier DW, Boisvert RF, Clark CW, editors. NIST Handbook of Mathematical Functions. Cambridge: Cambridge University Press; 2010. Chapter 8

[23] Autran JL, Glorieux M, Munteanu D, Clerc S, Gasiot G, Roche P. Particle Monte Carlo modeling of single-event transient current and charge collection in integrated circuits. Microelectronics Reliability. 2014;**54**:2278-2283

[24] Glorieux M, Autran JL, Munteanu D, Clerc S, Gasiot G, Roche P. Random-walk drift-diffusion charge-collection model for reverse-biased junctions embedded in circuits. IEEE Transactions on Nuclear Science. 2014;**61**:3527-3534

[25] Autran JL, Munteanu D, Moindjie S, Saad Saoud T, Malherbe V, Gasiot G, et al. Charge collection physical Modeling for soft error rate computational simulation in digital circuits. In: Sher Akbar N, Anwar Beg O, editors. Modeling and Simulation in Engineering Sciences. Vienna: London, UKIntechOpen; 2016 Chapter 6

[26] Plante I, Cucinotta FA. Monte-Carlo simulation of particle diffusion in various geometries and application to chemistry and biology. In: Chan VWK, editor. Theory and Applications of Monte Carlo Simulations. Vienna: London, UKIntechOpen; 2013

[27] Press WH, Teukolsky SA, Vetterling WT, Flannery BP, Metcalf M. Numerical Recipes in c: The Art of Scientific Computing. 2nd ed. Cambridge: Cambridge University Press; 1992

[28] Hazucha P, Svensson C. Impact of CMOS technology scaling on the atmospheric neutron soft error rate. IEEE Transactions on Nuclear Science. 2000;**47**:2586-2594